

Effective behavior of heterogeneous media governed by strain gradient elasticity

Harkirat Singh, Mayank Raj, Kaushik Bhattacharya*

Division of Engineering and Applied Sciences,
California Institute of Technology,
Pasadena CA 91125

July 8, 2025

Abstract

Various mechanical phenomena depend on the length scale, and these have inspired a variety of nonlocal and higher gradient continuum theories. Mechanistically, it is believed that the length scale dependence arises due to an interplay between the length scale of heterogeneities in the material, the length scale of the material being probed and the phenomenon under study. In this paper, we seek to understand this interplay in a simple setting by studying the overall behavior of a one-dimensional periodic medium governed by strain gradient elasticity at the microstructural scale. We find that the overall behavior is not described by a strain gradient elasticity. In other words, strain gradient theories are not invariant under averaging at this scale. We also find that the overall behavior may be described by a kernel-based nonlocal elasticity theory, and approximated locally by a fractional strain gradient elasticity. Consequently, one can obtain various scaling laws with exponent between zero (classical elasticity) and one (strain-gradient elasticity). We also learn the overall behavior using a Fourier neural operator.

1 Introduction

This paper is concerned with the overall behavior of heterogeneous materials where the underlying phenomenon depends on a length scale. We specifically consider a one-dimensional periodic medium governed by strain-gradient elasticity [14], and seek to understand the behavior on scales larger than the period. Müller and Francfort [32] showed that in the homogenized limit, where the ratio of the period to the overall domain goes to zero, the behavior is described by elasticity (with no dependence on the strain gradient and thus no scale dependence) where the effective elastic modulus depends on ratio of the material scale

*Corresponding author. Email: bhatta@caltech.edu

and microstructure scale. We are interested in the behavior when the ratio of the scale of application to the scale of microstructure is large, but finite, i.e., away from the asymptotic homogenized limit.

The continuum theory of elasticity with length scale dependence takes one of two approaches. The first is a nonlocal or “integral” approach (sometimes referred to as strongly nonlocal) where the stress at a point depends on strains across a domain via decaying kernel functions [13, 11, 12]. Such theories have been used to study (dispersive) wave propagation and defects like screw dislocations [14]. The second is the “gradient” approach (sometimes referred to as weakly nonlocal) wherein the stress is a function of the strain and its gradients at the same point [14]. Such theories have been used to regularize singular solutions of classical elasticity, for example at crack tips [39, 40]. However, these theories are all postulated phenomenologically at the macroscopic scale.

It is possible to derive nonlocal theories, especially strain gradient theories, starting from either discrete models using dispersion relations [25, 24], or heterogeneous materials using ‘higher order homogenization’ [6]. A subtle issue that arises in the latter is that the truncation of the expansion at second order requires care and a naive truncation can lead to a non-positive-definite second-order modulus [3, 36, 38].

There are a number of observations of the dependence of mechanical properties on material scales, especially in plastic yield. The seminal work is due to Hall [19] and Petch [35] who showed that the yield strength increased with the inverse of the square-root of the grain size (smaller is stronger), and attributed this to dislocation pile-up at grain boundaries. Fleck *et al.* [16] observed that the hardening in wires under torsion depends on the wire diameter while Nix and Gao [33] observed length scale dependence in indentation; also [10] for a summary. All of this has motivated a very rich literature on gradient theories of plasticity [2, 16, 33, 15, 18]. Further scale effects have been observed in plasticity since the advent of nano-pillar compression [17, 30, 31]. A key conclusion of the newer observations is that the scaling law (the exponent in the strength or hardening vs. length scale) can vary widely depending on circumstance, and none of the gradient theories are able to predict these exactly. This motivated Dahlberg and Ortiz [8] to propose a fractional strain gradient plasticity. However, all of this modeling effort is macroscopic and phenomenological. At the same time, the underlying mechanism for the length scale dependence is related to heterogeneities [4]. Therefore, it would be interesting to understand the length scale dependence starting from a heterogeneous medium, and this is the motivation for the current work.

In this paper, we study a simple problem of a one-dimensional heterogeneous medium governed by strain gradient elasticity at the microstructural scale, and characterize the overall behavior on scales that are large compared to the microstructural scale. We find that the overall behavior is not described by strain gradient elasticity. In other words, strain gradient theories are not invariant under change of scale. We also find that the overall behavior may be described by a kernel-based nonlocal elasticity theory, and approximated locally by a fractional strain gradient elasticity. Consequently, one can obtain various scaling laws with exponent between zero (classical elasticity) and one (strain-gradient elasticity). We also learn the overall behavior using a Fourier neural operator [26, 23, 7].

The paper is organized as follows. We introduce our one-dimensional strain gradient theory in Section 2, and describe methods we use to solve problems in Section 3. We gain insight into strain gradient elasticity by studying a hanging bar (a bar fixed at one end and

subjected to uniform body force) in Section 4. The heart of the paper is Section 5 where we study an infinite bar subjected to periodic forcing. Section 6 describes operator learning. We conclude in Section 7.

2 Strain-gradient elasticity

We consider a bar of length \tilde{L} and uniform cross-section \tilde{A} , possibly made of a periodic microstructure with unit cell length \tilde{l} . The elastic modulus is \tilde{E} , and the strain gradient modulus is $\tilde{\kappa}$. We have an imposed body force per unit length \tilde{f} . The total energy in the system undergoing displacement \tilde{u} is

$$\frac{1}{2} \int_0^{\tilde{L}} \tilde{A} \left(\tilde{E} \tilde{u}_{\tilde{x}}^2 + \tilde{\kappa} \tilde{u}_{\tilde{x}\tilde{x}}^2 - \tilde{f} \tilde{u} \right) d\tilde{x} + \tilde{\mathcal{B}}, \quad (1)$$

where $\tilde{\mathcal{B}}$ depends on the boundary condition. Note that $\tilde{E}, \tilde{\kappa}$ may be heterogeneous (periodic). It is convenient to non-dimensionalize using a reference length \tilde{L}_0 for length and a reference modulus \tilde{E}_0 for energy density ($\tilde{E}_0 \tilde{L}_0^2$ for $\tilde{\kappa}$ and $\tilde{E}_0 / \tilde{L}_0$ for \tilde{f}). We denote the non-dimensional quantities by the name letters without the tilde. The energy now is

$$\mathcal{E}(u) = \frac{1}{2} \int_0^1 A (E u_x^2 + \kappa u_{xx}^2 - f u) dx + \mathcal{B} = \frac{1}{2} \int_0^1 A (E (u_x^2 + \lambda^2 u_{xx}^2) - f u) dx + \mathcal{B} \quad (2)$$

where $\lambda = \sqrt{\kappa/E}$ is the (non-dimensional) material length. The corresponding equilibrium equation is

$$(E u_x - (\lambda^2 E u_{xx})_x)_x + f = 0, \quad (3)$$

and the jump conditions are

$$[[u]] = 0, \quad [[u_x]] = 0, \quad [[E u_x - (\kappa u_{xx})_x]] = 0, \quad [[\kappa u_{xx}]] = 0. \quad (4)$$

as shown in Appendix A. Note that we have two stresses, the Cauchy stress $E u_x - (\kappa u_{xx})_x$ and a higher order stress κu_{xx} . We need to add appropriate boundary conditions.

We study two problems in the following sections.

Hanging bar. A bar is suspended from one end, free at the other and subject to a uniform body force. So, we set the displacement to be zero on one end, the stress to be zero at the other, and the higher order stress to be zero on both ends:

$$u(0) = u_{xx}(0) = 0, \quad u_{xx}(L) = (E u_x - (\kappa u_{xx})_x)(L) = 0, \quad f = f^* \quad (5)$$

where f^* is a constant.

We consider two problems with different microstructures. The first is a homogeneous bar where E and κ are uniform. The second is a periodic bar made of two materials,

$$E(x) = \begin{cases} E_1 & 0 \leq \{x/l\} < 1/2 \\ E_2 & 1/2 \leq \{x/l\} < 1 \end{cases}, \quad \kappa(x) = \begin{cases} \kappa_1 & 0 \leq \{x/l\} < 1/2 \\ \kappa_2 & 1/2 \leq \{x/l\} < 1 \end{cases} \quad (6)$$

where $\{y\}$ denotes the fractional part of y (the difference between y and the largest integer smaller than y), l is the period and $N = L/l$ is the number of unit cells.

Infinite bar subjected to periodic forcing. This is an infinite two-material bar with periodic moduli given by (6) and subject to a periodic body force

$$f(x) = \sin kx \quad (7)$$

where k is the wave number of the load (equivalently $\ell = 2\pi/k$ is the period or wavelength of loading). We take $\ell/l = 2\pi/kl$ to be rational (a/b for a, b positive integers) and greater than one, so that both the microstructure and loading can be periodic with period $p = abl$. Therefore, we can look for p -periodic solutions to (3) subject to $\langle u \rangle = 0$.

3 Methods

3.1 Transfer matrix method

We seek to solve (3) on $(0, L)$ where the moduli is piecewise constant

$$E(x) = E_i, \quad \kappa(x) = \kappa_i \quad x \in (x_{i-1}, x_i), \quad i = 1, \dots, I \quad (8)$$

where $x_0 = 0 < x_1 < \dots < x_I = L$ and some boundary conditions at $x = 0, L$ using a transfer matrix method [20, 22]. In each segment (x_{i-1}, x_i) , it is easy to verify that the homogeneous solution to (3) is given by

$$u(x) = c_1 \exp\left(\frac{x}{\lambda_i}\right) + c_2 \exp\left(-\frac{x}{\lambda_i}\right) + c_3 x^2 + c_4 x \quad (9)$$

Set $\varphi_i = (u, u_x, Eu_x - (\kappa u_{xx})_x, \kappa u_{xx})^T$ in the i^{th} segment. Using the solution above, we may write

$$\varphi_i(x_{i-1}) = \Phi_i(x_{i-1})C + \varphi_i^p(x_{i-1}), \quad \varphi_i(x_i) = \Phi_i(x_i)C + \varphi_i^p(x_i), \quad (10)$$

where Φ is the matrix given in Appendix B and $C = (c_1, c_2, c_3, c_4)^T$. φ^p is obtained from the particular solution depending on f , and expressions for constant and sinusoidal f are given in Appendix B. Eliminating C , we find

$$(\varphi_i(x_i) - \varphi_i^p(x_i)) = T_i (\varphi_i(x_{i-1}) - \varphi_i^p(x_{i-1})) \quad (11)$$

where $T_i = \Phi_i(x_i)\Phi_i(x_{i-1})^{-1}$ is the transfer matrix in the i^{th} segment.

Now, the jump conditions (4) implies that φ is continuous, i.e., $\varphi_i(x_{i-1}) = \varphi_{i-1}(x_{i-1})$. We can use this to infer that

$$\begin{aligned} (\varphi_i(x_i) - \varphi_i^p(x_i)) &= T_i (\varphi_{i-1}(x_{i-1}) - \varphi_{i-1}^p(x_{i-1})) - T_i [[\varphi^p(x_{i-1})]] \\ &= T_i T_{i-1} (\varphi_{i-1}(x_{i-2}) - \varphi_{i-1}^p(x_{i-1})) - T_i [[\varphi^p(x_{i-1})]] \\ &= T_i T_{i-1} T_{i-2} (\varphi_{i-2}(x_{i-3}) - \varphi_{i-2}^p(x_{i-3})) \\ &\quad - T_i T_{i-1} [[\varphi^p(x_{i-2})]] - T_i [[\varphi^p(x_{i-1})]] \\ &= (\Pi_{\alpha=0}^i T_\alpha) (\varphi_1(0) - \varphi_1^p(x_0)) - \sum_{\beta=1}^i (\Pi_{\alpha=\beta}^i T_\alpha) [[\varphi^p(x_{\alpha-1})]]. \end{aligned} \quad (12)$$

Above, we apply continuity of φ at x_{i-1} to obtain the first equality, the analog of (11) for $i - 1$ to obtain the second and so forth. Setting $i = I$, the relationship (12) enables us to relate $\varphi(L)$ to the solution at $\varphi(0)$ by. Since four of these eight quantities are known from the boundary conditions, we may regard this as a set of linear equations for the remaining unknowns.

We can also use the transfer matrix method in the periodic setting by setting $\varphi(L) = \varphi(0)$ from periodicity and solving (12) for $\varphi(0)$.

3.2 Fast Fourier transfer method

We consider a periodic domain and a periodic forcing f . We follow Moulinec and Suquet [27, 28] and others (see [29] for a recent review) to look for a periodic solution to the governing equation (3) using a Lippmann-Schwinger type iterative method,

$$E_0 u_{xx}^{n+1} - \kappa_0 u_{xxxx}^{n+1} = -f - ((E - E_0)u_x^n)_x + ((\kappa - \kappa_0)u_{xx}^n)_{xx} =: \mathcal{F}^n, \quad (13)$$

where $E_0 > 0, \kappa_0 > 0$ are uniform constants. Taking the Fourier transform,

$$(-k^2 E_0 - k^4 \kappa_0) \hat{u}^{n+1}(k) = \hat{\mathcal{F}}^n(k) \quad \implies \quad \hat{u}^{n+1}(k) = \frac{\hat{\mathcal{F}}^n(k)}{(k^2 E_0 + k^4 \kappa_0)} \quad (14)$$

where k is the variable in the Fourier domain.

Given u^n and its derivatives, we compute \mathcal{F}^n in real space and then use fast Fourier transform (FFT) to compute $\hat{\mathcal{F}}^n$. This enables the calculation of \hat{u}^{n+1} ; an inverse FFT provides u^{n+1} . We iterate in this manner till we converge according to the criteria,

$$r_1 = \|u^{n+1} - u^n\| \leq r_1^{\text{tol}}, \quad r_2 = \|u_{xx}^{n+1} - u_{xx}^n\| \leq r_2^{\text{tol}} \quad (15)$$

for given tolerances $r_1^{\text{tol}}, r_2^{\text{tol}}$.

3.3 Bloch-Floquet theory

In a periodic setting where the forcing has a larger period than the unit cell, we can invoke the Bloch-Floquet theorem that a $2\pi/k$ periodic function u may be represented as

$$u(x) = v(x)e^{ikx}, \quad (16)$$

where $v(x)$ is l -periodic (e.g., [5]). We can use this in both the transfer matrix and fast Fourier transform method to solve the problem on the unit cell.

4 Hanging bar

The lengths in this section are normalized by the length L of the bar.

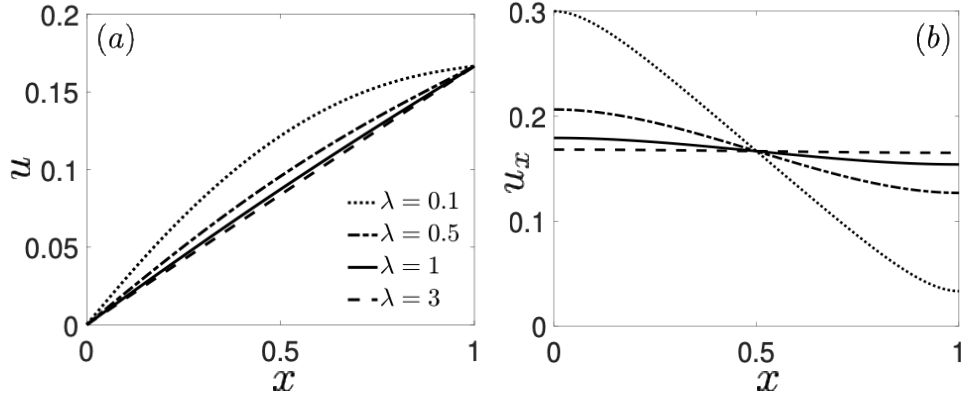


Figure 1: Displacement (a) and strain (b) in a homogeneous hanging bar for various material length scales λ .

4.1 Homogeneous bar

We solve (3) subject to the boundary condition and body force (5). It is easy to verify that the solution is given by

$$u(x) = \frac{f^* \lambda^2}{E} \left(\frac{e^{x/\lambda}}{1 + e^{L/\lambda}} + \frac{e^{-x/\lambda}}{1 + e^{-L/\lambda}} - 1 \right) + \frac{f^*}{2E} (2Lx - x^2) \quad (17)$$

Figure 1 displays the displacement and strains for various values of material length $\lambda = \sqrt{E/\kappa}$. Note that these depend on the material length. Still, the end displacement, $u(L) = f^* L^2 / 2E$, is independent of the higher order modulus κ , and thus the material length.

4.2 Heterogeneous bar

We now consider the same problem but with the moduli are given by (6). We solve it using the transfer matrix method. For future use, we denote the quantity

$$\bar{E} = \frac{f^* L^2}{2u(L)} \quad (18)$$

the *effective elastic modulus* motivated by the relation between the modulus and end displacement in the case of the homogenous bar.

We start with the case of a two-piece bar where $l = L$ ($N = l/L = 1$) and fix $E_1 = 1$, $E_2 = 5$. Figure 2(a) shows the strain for various combinations of material lengths λ_1 and λ_2 . We see the effect of the interface, and its dependance on the material lengths. The effective modulus \bar{E} (cf. (18)) is shown in Figure 2(b). In contrast to the case of the homogeneous bar, the effective modulus of the two-piece bar depends on the material scales due to the presence of the boundary layers near the interface. When both the material lengths are large, the boundary layer dominates the bar and so the effective elastic modulus approaches arithmetic mean of the two elastic moduli ($\bar{E} = \langle E \rangle$ where $\langle \cdot \rangle$ denotes the average). In contrast, when either or both material lengths are small, the boundary layer at the interface is small and

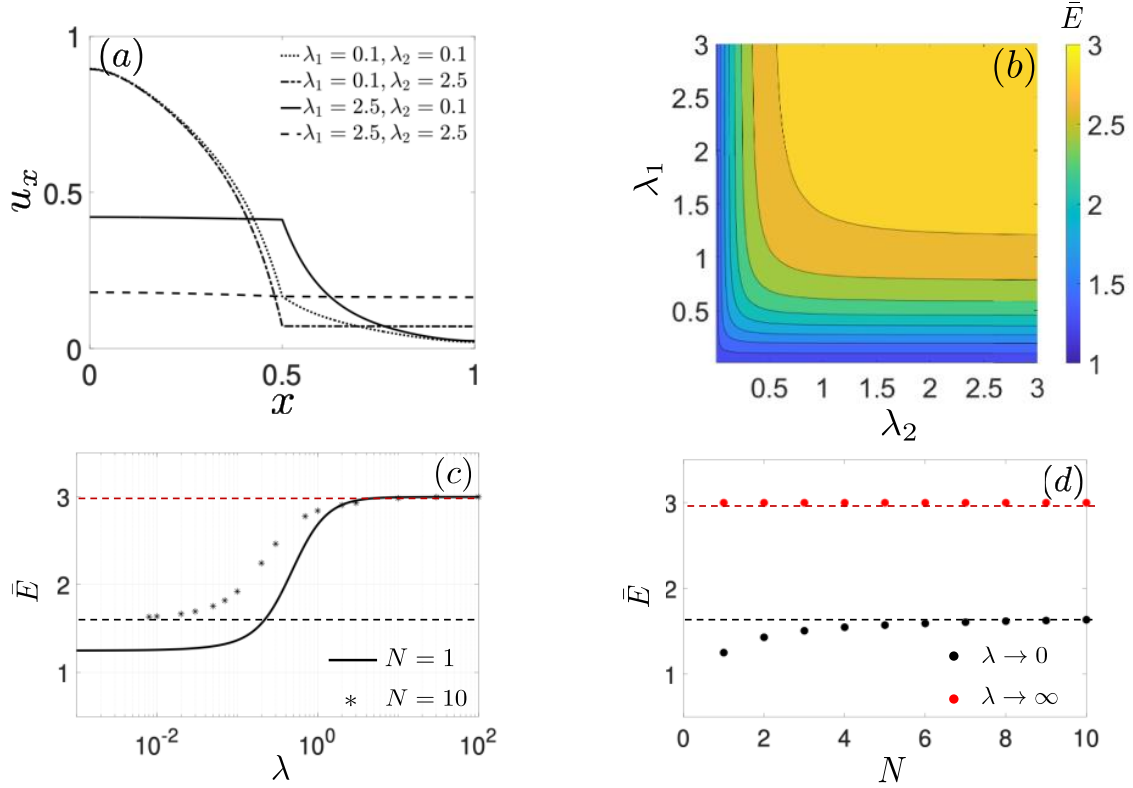


Figure 2: Strain and effective elastic modulus of a heterogeneous bar with $E_1 = 1$ and $E_2 = 5$. (a) Strain in a two-piece bar ($N=1$) for various combinations of material lengths. (b) Effective elastic modulus of a two-piece bar ($N=1$) for various combinations of material lengths. (c) Effective elastic modulus for $N = 1, 10$ as a function of the material length when $\lambda_1 = \lambda_2 = \lambda$. (d) Effective elastic modulus as a function of N for large and small material length ($\lambda_1 = \lambda_2$).

we approach the elastic solution. In fact, when $\lambda_1 = \lambda_2 = \lambda$, we can show that

$$\bar{E}(\lambda) = \frac{15}{4} \left(3 - 6\lambda^2 + 6\lambda^2 \operatorname{sech} \left(\frac{1}{2\lambda} \right) - 2\lambda \tanh \left(\frac{1}{2\lambda} \right) \right)^{-1}. \quad (19)$$

This is shown in the Figure 2(c) as the solid line.

We generalize to a periodic bar with N periods in the case of equal material lengths, $\lambda_1 = \lambda_2 = \lambda$. Figure 2(c) shows the effect of λ for the cases $N = 1, 10$. We see that when N is large, the effective elastic modulus interpolates between the harmonic and arithmetic means. This is consistent with the analysis of Müller and Francfort [32]. However, this figure also shows that there is a dependence on the number of periods N .

Figure 2(d) shows how the effective elastic modulus changes with the number of periods N in the bar for large and small material lengths. When the material lengths are large, the boundary layer dominates and the effective elastic modulus remains close to the arithmetic mean with no significant dependence on the number of segments. In contrast, when the material lengths are small, we see that the effective modulus increases with the number of segments. To understand this, recall that we approach the elastic solution. Since $E_1 < E_2$,

we have a larger strain in the first segment even though it has a smaller stress under uniform body force. This effect diminishes with the number of segments, and the effective elastic modulus approaches the harmonic mean $\bar{E} = \langle E^{-1} \rangle^{-1}$ corresponding to a purely elastic bar.

The analysis of Müller and Francfort [32] studies the case where specimen is large compared to the microstructure and material scale. However, Figures 2(c) and (d) show that there is a strong interplay between the material scale (λ), the microstructure scale (l) and the scale of specimen L . We explore this further in the next Section.

5 Infinite bar subjected to periodic forcing

The lengths in this section are normalized by the period l .

5.1 Homogeneous bar

Consider an infinite homogeneous bar subjected to periodic body force $f = \sin kx$. It is easy to see that the solution is given by

$$u(x) = \frac{\sin(kx)}{Ek^2 + \lambda^2 Ek^4}. \quad (20)$$

The solution scales as k^{-2} when k is small (the forcing is slowly varying), and k^{-4} when k is large (the forcing is rapidly varying).

5.2 Heterogeneous bar

We now consider the same problem but with the moduli distribution given by (6). We normalize all lengths with the period l . We only consider wave numbers $k < 2\pi$ so that the loading wave-length is larger than the unit cell. We fix $E_1 = 1, E_2 = 5$. We solve the problem (3) using both the transfer matrix method and fast Fourier transform method, and verify that they result in the same solution.

Figure 3(a) shows the displacement and strain for four cases of material length combinations, with $k = \pi/2$. We observe that the dominant response is at the wave number $k = \pi/2$, but also has finer oscillations due to the heterogeneity. We focus on the dominant response. Indeed, since (3) is linear and elliptic, we expect that we can write the solution as

$$u(x) = (G * f)(x) = \int G(x - y)f(y)dy \quad (21)$$

for a Green's function G . Taking the Fourier transform,

$$\hat{u}(k) = \hat{G}(k)\hat{f}(k) \quad (22)$$

The invariance ($f(x) \rightarrow f(-x) \implies u(x) \rightarrow u(-x)$) due to frame-indifference implies that \hat{G} is real, and hence G is symmetric about the origin.

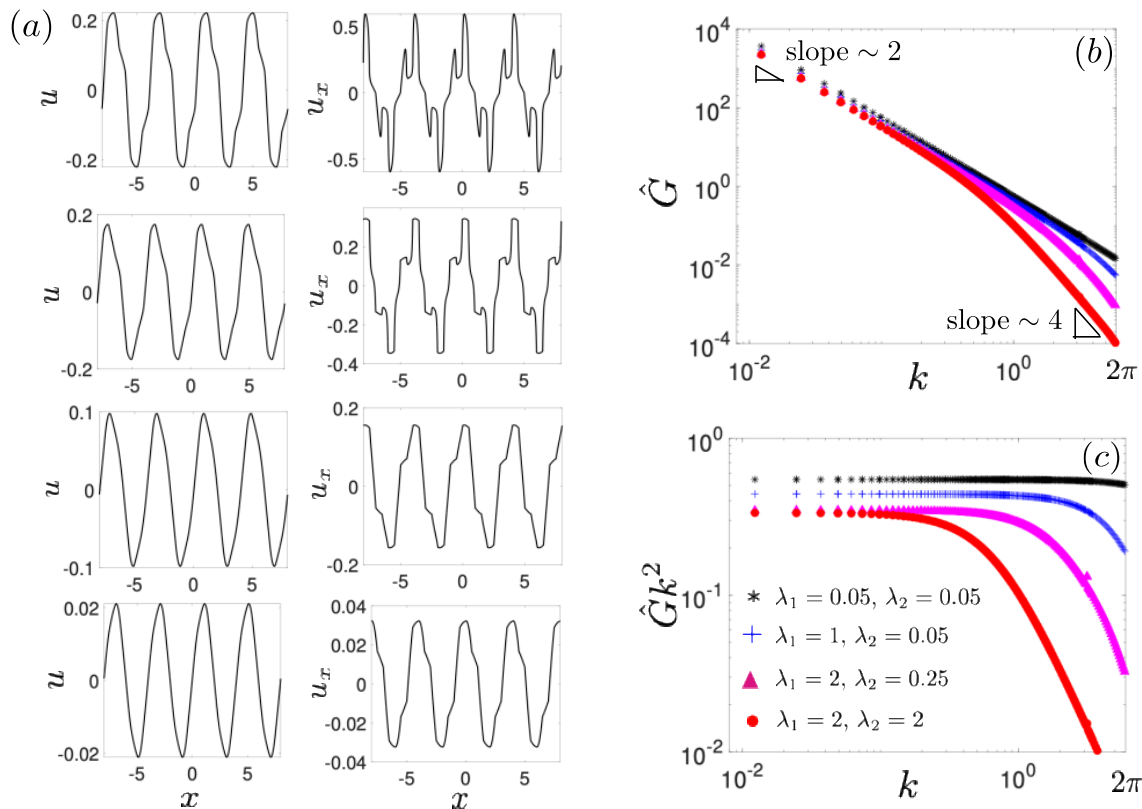


Figure 3: Response of a periodic heterogeneous bar subjected to sinusoidal loading (a) Displacement and strain over four loading wavelengths with $k = \pi/2$, (b) Amplification \hat{G} and (c) $\hat{G}k^2$ for various material length scales. All figures have the same values and order as in part(c).

Overall response Figure (3)(b) shows the response \hat{G} as a function of the wave number k at scales larger than the unit cell for four combinations of material scales. Note that this figure is plotted on a logarithmic scale. In all the cases, the large length scale limit has a slope of 2. It follows,

$$-\lim_{k \rightarrow 0} \frac{d \log \hat{G}}{d \log k} = 2 \iff \hat{G} \approx \frac{1}{\bar{E}k^2} \text{ for small } k \quad (23)$$

This is emphasized in Figure (3)(c) that shows $\hat{G}k^2$ as a function of k . We conclude that the long wavelength limiting behavior is elasticity for some effective elastic modulus \bar{E} . This is consistent with the analysis of Müller and Francfort [32], and our results in the hanging bar. We will study \bar{E} in detail later.

Figure (3)(b) also shows that the slope approaches 4 for large k when the material lengths are large. This is because the gradient term dominates the response in this regime.

Effective theory In light of these two limiting cases, and also comparing the response of the heterogeneous and homogeneous materials, it is natural to seek an effective response

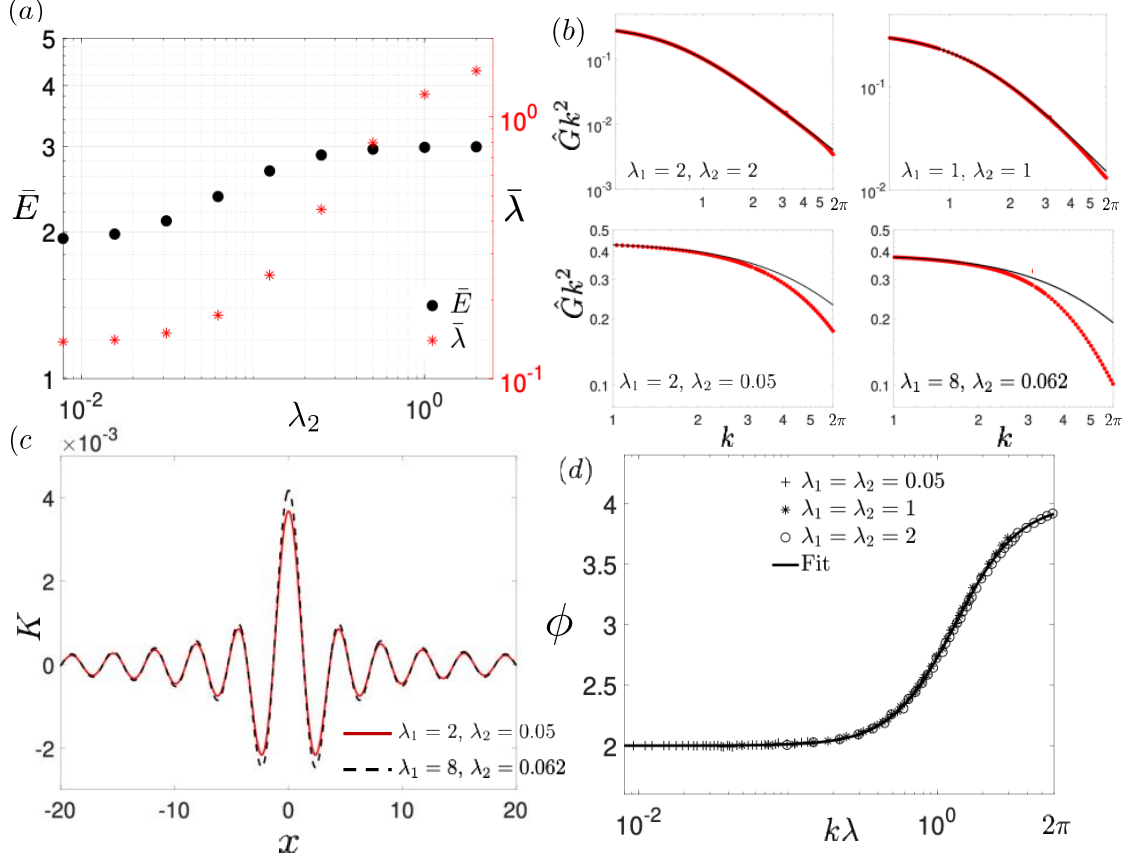


Figure 4: The effective response of a heterogeneous bar. (a) The best fit effective elastic modulus \bar{E} and effective material length $\bar{\lambda}$ as a function of the material length λ_2 with $\lambda_1 = 2$. (b) Comparison between the best effective strain gradient elasticity and actual response. (c) The kernels of non-local elasticity that describe the effective behavior a few combination of material lengths and (d) Empirical relationship between the exponent ϕ (cf. (29) and scaled wavenumber λk . $E_1 = 1, E_2 = 5$ in all these figures.

with an effective elastic modulus \bar{E} and effective material length $\bar{\lambda}$, or

$$\hat{G} \approx \frac{1}{\bar{E}k^2 + \bar{\lambda}^2 \bar{E}k^4} \quad (24)$$

We fit \bar{E} from the intercept of Figure (3)(c) (cf. (23)), and $\bar{\kappa} = \bar{\lambda}^2 \bar{E}$ by a least-square fit of (24) in the range $(0, 2\pi)$. The results are shown in Figure 4(a) a function of λ_2 when $\lambda_1 = 2$. The elastic modulus \bar{E} varies from the harmonic mean to the arithmetic mean consistent with the results of Müller and Francfort [32], and our results in the hanging bar. The effective material length $\bar{\lambda}$ increases with λ_2 : still, note that $\bar{\lambda} \neq 2$ even when $\lambda_1 = \lambda_2 = 2$. This is because our elastic modulus is not uniform. In other words, heterogeneous elastic modulus affects the effective material length.

We compare the best effective strain gradient elasticity theory according to (24) with the computed effective response in Figure 4(b). We see reasonable agreement when the two material lengths are the same, but see a deviation when the material lengths are different.

Thus, *the effective behavior of a heterogeneous strain gradient elastic medium is not described by a strain gradient elastic theory.* In other words, the interaction between the different material lengths give rise to interactions that are not described by a strain gradient theory.

Nonlocal elasticity A more general representation is given by a non-local elasticity theory [12] where the stress at a point depends on an integral of the strain

$$\sigma(x) = \bar{E}\varepsilon(x) + (K * (K * \varepsilon))(x) = \bar{E}\varepsilon(x) + \int K(x-z) \int K(z-y)\varepsilon(y)dy dz \quad (25)$$

for a suitable kernel K . The corresponding equilibrium equation is

$$(\bar{E}u_x + K * (K * u_x))_x + f = 0. \quad (26)$$

Taking Fourier transform of this equation and recalling the definition of the Green's function, we can calculate the Fourier transform of the kernel in terms of the Fourier transform of the Green's function

$$\hat{G} = \frac{1}{k^2(\bar{E} + \hat{K}^2)} \iff \hat{K} = \left(\frac{1}{\hat{G}k^2} - \bar{E} \right)^{1/2}. \quad (27)$$

We can now use our results to obtain the Fourier transform of the kernel, and then the kernel. The result is shown in Figure 4(c) for a few combinations of material scales.

Fractional strain derivative elasticity While we see a complex behavior over the entire range of length scales large compared to the unit cell, we are often interested in a narrower range of length scales. Indeed many experiments on length scale effects are limited to factors of two to five. In this situation, it is natural to look for the response in this limited range of length scales. We do so by linearizing the relationship between the Fourier transform of the Green's function \hat{G} and wave number k in the logarithmic scale,

$$\log \hat{G}(k) \approx \log \hat{G}(k_0) - \phi(k_0)(\log k - \log k_0) \quad (28)$$

where

$$\phi(k) := -\frac{d \log \hat{G}}{d \log k}(k). \quad (29)$$

We find empirically that $\phi \in (2, 4)$ and fits the relationship

$$\phi(k) = 2 + 2 \left(\left(\frac{R_{\text{tr}}}{\bar{\lambda}k} \right)^m + 1 \right)^{-1}. \quad (30)$$

where $\bar{\lambda}$ and m are fitting parameters, and $R_{\text{tr}} = 0.212$. This relationship is shown in Figure 4(d), and the fitting parameters for some cases are listed in Table 1. In the case when $\lambda_1 = \lambda_2$, we find that $\bar{\lambda} = \lambda_1 = \lambda_2$, $m = 2$.

Returning to (28), we can rewrite it as

$$\hat{G}(k) \approx \hat{G}(k_0) \left(\frac{k}{k_0} \right)^{-\phi(k_0)} = \frac{C}{2M\bar{\lambda}^{\phi-2}k^\phi}. \quad (31)$$

λ_1	λ_2	λ	m
λ	λ	λ	2
1	0.05	0.048	3.27
8	0.0625	0.0541	3.82

Table 1: Fitting parameters in the universal relationship between the exponent ϕ and wavenumber k . $E_1 = 1, E_2 = 5$.

for some effective modulus M (with units of energy per volume) and some effective material length $\bar{\lambda}$. C is a constant that depends only on ϕ and enters through the derivation of the fractional derivative and fractional Laplacian.

The theory of fractional calculus is quite intricate [1, 37], and we refer the reader to Di Nezza *et al* [9] for an easily accessible introduction. We define the fractional Laplacian of order $\alpha \in (0, 1)$ as

$$(-\Delta)^\alpha u := C \int_0^L \left(\frac{u'(x) - u'(y)}{|x - y|^{1+2\alpha}} \right) dy. \quad (32)$$

where the constant C depends only α . Taking Fourier transform [9],

$$\widehat{(-\Delta)^\alpha u} = -|k|^{2\alpha} \hat{u}. \quad (33)$$

Therefore, (31) is equivalent to the equilibrium equation

$$\sigma_x + f = 0, \quad \sigma = \frac{2M\bar{\lambda}^{2\alpha}}{C} (-\Delta)^\alpha \varepsilon \quad \text{where} \quad \alpha = \frac{\phi - 2}{2} \in (0, 1) \quad (34)$$

and $\varepsilon = u_x$ is the strain. Thus, the stress is linear in the α^{th} fractional Laplacian.

Equivalently, as shown in Appendix D, we can pose the equilibrium problem as one of minimizing the total energy where the total energy is defined using the α -fractional derivative through the Gagliardo 2-semi-norm,:

$$\min_u \mathcal{E}(u), \quad \mathcal{E}(u) = \int_0^L A \left(\int_0^L \frac{1}{2} M \bar{\lambda}^{2\alpha} \frac{(u'(x) - u'(y))^2}{|x - y|^{1+2\alpha}} dy - f(x)u(x) \right) dx + \mathcal{B} \quad (35)$$

where \mathcal{B} depends on the boundary condition.

We now use this variational formulation to study a simple problem where a bar is subjected to dead load to understand the resulting scaling law. The approach follows a calculation by Dahlberg and Ortiz [8]. We take $f = 0$, and $\mathcal{B} = A\sigma(u(L) - u(0)) = A\sigma \int_0^L u'(x) dx$ corresponding to a dead traction σ at the ends of the bar. Substituting this in (35), we have

$$\begin{aligned} \min_u \mathcal{E}(u) &= \min_\varepsilon \int_0^L A \left(\int_0^L \frac{1}{2} M \bar{\lambda}^{2\alpha} \frac{(\varepsilon(x) - \varepsilon(y))^2}{|x - y|^{1+2\alpha}} dy - \sigma \varepsilon(x) \right) dx \\ &= AL \min_\varepsilon \int_0^1 \left(\frac{1}{2} M \bar{\lambda}^{2\alpha} L^{-2\alpha} \int_0^1 \frac{1}{2} \frac{(\varepsilon(\bar{x}) - \varepsilon(\bar{y}))^2}{|\bar{x} - \bar{y}|^{1+2\alpha}} d\bar{y} - \sigma \varepsilon \right) d\bar{x} \end{aligned} \quad (36)$$

Now, given any $\varepsilon(x)$, let $\bar{\varepsilon} = (\int_0^1 \varepsilon(\bar{x}) d\bar{x})$, and $\tilde{\varepsilon} = \varepsilon/\bar{\varepsilon}$, so $\varepsilon = \bar{\varepsilon} \tilde{\varepsilon}$ with $\int_0^1 \tilde{\varepsilon} d\bar{x} = 1$. Note that $\bar{\varepsilon} = (\int_0^L \varepsilon(x) dx)/L$ is the average strain in the bar. Substituting this back, we find

$$\min_u \mathcal{E}(u) = \min_{\bar{\varepsilon}} AL \left(\frac{1}{2} M \bar{\lambda}^{2\alpha} L^{-2\alpha} \bar{\varepsilon}^2 D - \sigma \bar{\varepsilon} \right) \quad (37)$$

where

$$D = \min_{\{\bar{\varepsilon}: \int_0^1 \bar{\varepsilon} d\bar{x}=1\}} \int_0^1 \frac{(\varepsilon(\bar{x}) - \varepsilon(\bar{y}))^2}{|\bar{x} - \bar{y}|^{1+2\alpha}} d\bar{x} \quad (38)$$

is independent of L . We conclude from (37) that the average strain

$$\bar{\varepsilon} = \frac{\sigma}{MD} \left(\frac{\bar{\lambda}}{L} \right)^{2\alpha} \quad (39)$$

will depend on the size with exponent 2α . When $\alpha = 0$, there is no dependence on the length corresponding to classical elasticity, and when $\alpha = 1$ we have quadratic dependence corresponding to purely strain gradient elasticity. In general, $\alpha \in (0, 1)$ and we have an intermediate scaling law.

In summary, we conclude that *the effective behavior of a heterogeneous strain gradient elastic medium can be approximated by a fractional strain gradient elasticity in a limited range of length scales. Consequently, the effective behavior of a heterogeneous strain gradient elastic medium can display various scaling exponents between zero and one.*

6 Operator learning

We conclude this work by showing that a Fourier neural operator (FNO) is able to learn the overall response of the material. We specialize to the case of equal material scales, $\lambda_1 = \lambda_2 = \lambda$, and seek to learn the operator $\{f, \lambda\} \rightarrow u$.

6.1 Fourier neural operator

A Fourier neural operator (FNO) [26, 23, 7] is an operator $i \rightarrow o$ where

$$o = (\mathcal{Q} \circ \sigma_N(v_{N-1}) \circ \cdots \circ \sigma_n(v_{n-1}) \circ \cdots \circ \sigma_1(v_0) \circ \mathcal{P}) i, \quad (40)$$

where $\{\sigma_n\}$ are activation functions, $v_n := W_n v_{n-1} + \mathcal{F}^{-1}(R_n) \mathcal{F} v_{n-1} + b_n$, \mathcal{P}, \mathcal{Q} are lifting and projection mappings, \mathcal{F} and \mathcal{F}^{-1} denote Fourier and inverse Fourier transforms and the parameters $P = \{W_n, R_n, b_n\}$. Universal approximation theorems have been established when the input and output spaces are Sobolev spaces, and the efficacy demonstrated in Navier-Stokes [23] and in elliptic problems [7].

In this work, we use the GeLU activation function and Adam optimizer for training [21], and implement it in the package PyTorch [34]

6.2 Learning the linear response

We begin with the linear map $f \rightarrow u$. We use three hidden Fourier layers with 256 Fourier modes and 64 channels in each layer. We generate 600 samples $(\{f, u\})$ by choosing a random forcing f and computing the resulting u at a resolution of 1024. The training and test errors over 2000 epochs are shown in Figure 5(a). Figure 5(b) compares the computed (truth) and predicted displacements for four test instances (these were not used in the training). An important property of FNOs is that it learns the operator and not the discretized map even

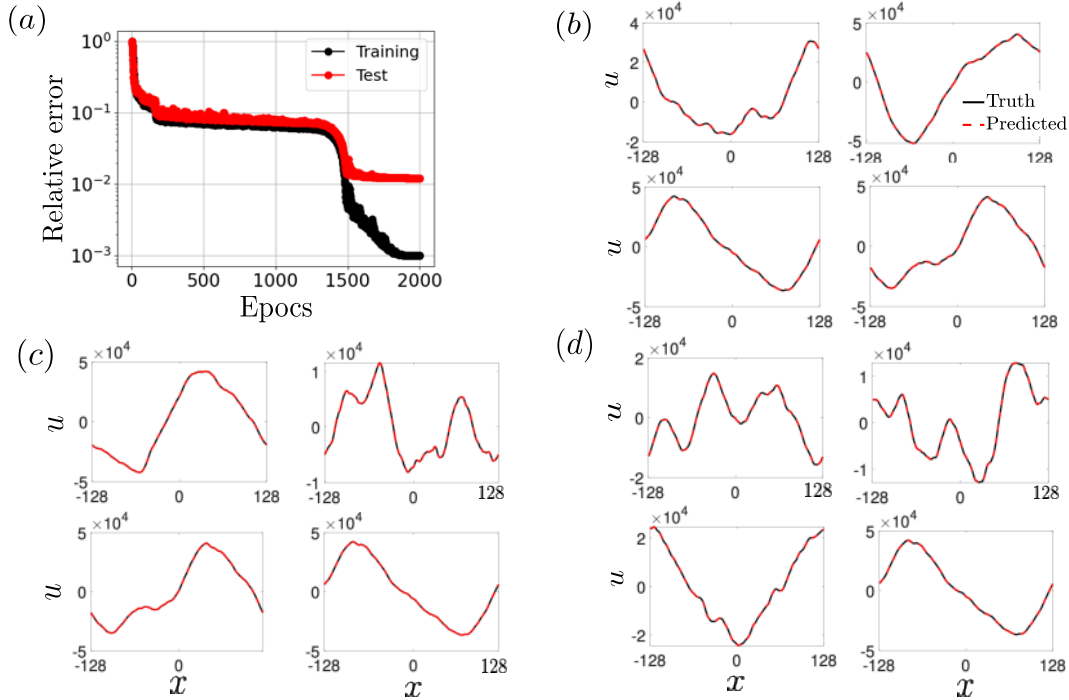


Figure 5: Learning the linear map. (a) Training and test error. (b) Comparison for four instances of test data. (c) Comparison for four instances of test data generated at a higher resolution than that used for training. (d) Comparison for four instances of test data generated at a lower resolution than that used for training. $E_1 = 1, E_2 = 5$.

though it is trained on discretized data. This is shown in Figures 5(c) and (d) where the already trained FNO is evaluated against data generated at a resolution of 4096 and 512 respectively. We have also verified linearity and the ability of the FNO to reproduce $\hat{G}(k)$.

6.3 Learning the material and response

Figure 6 shows the results for the nonlinear map $\{f, \lambda\} \rightarrow u$. We create a dataset of 2500 samples with 500 each at $\lambda = 2, 1, 0.5, 0.25, 0.05$. We pick 2000 samples for training for 2000 epochs. Figure 6(a) shows the training error while Figure 6(b) compares four test samples. Figure 6(c) compares the computed spectrum of the Green's function $\hat{G}(k)$ (truth) with that predicted by the FNO. We use the remaining 500 samples for testing the learnt model. We see excellent match showing that the FNO is able to learn the effect of the material length scale.

7 Conclusion

Motivated by the observation that nonlocal theories are a result of heterogeneity, we have studied a simple problem of a one-dimensional heterogeneous medium governed by strain gradient elasticity at the microstructural scale. We have characterized the overall behavior on scales that are large compared to the microstructural scale. We show that the overall behavior

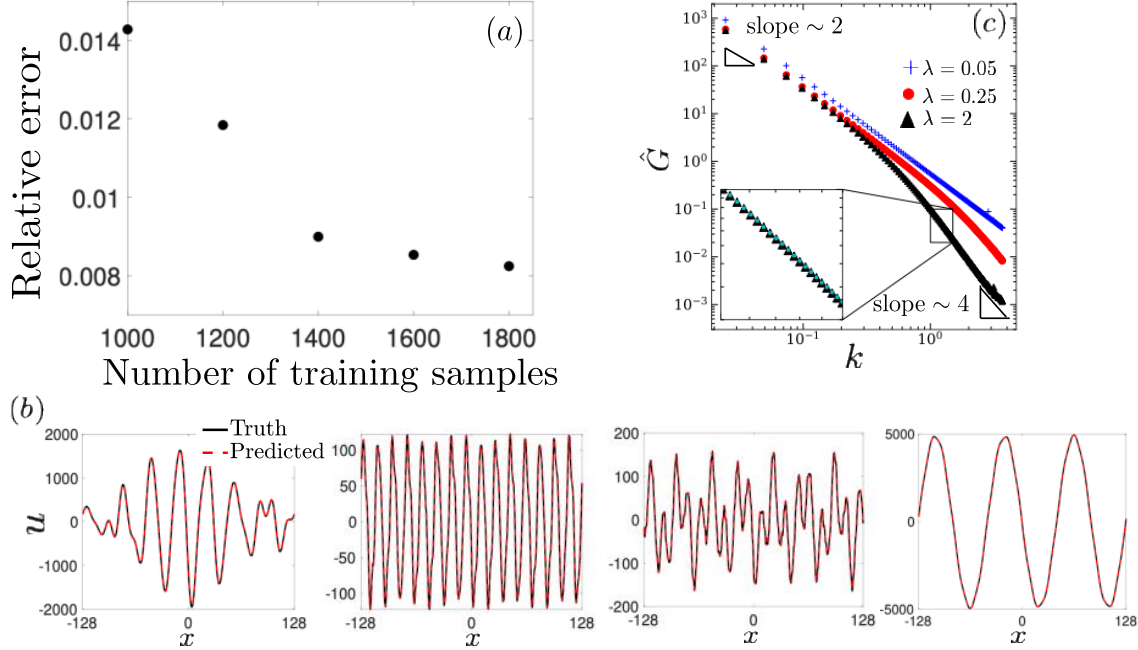


Figure 6: Learning the non-linear map. (a) Training and test error. (b) Comparison for four instances of test data. (c) Comparison of the Fourier transform of the Green’s function. $E_1 = 1, E_2 = 5$.

is not described by strain gradient elasticity. In other words, strain gradient theories are not invariant under change of scale. We also show that the overall behavior may be described by a kernel-based nonlocal elasticity theory, and locally approximated by a fractional strain gradient elasticity. Consequently, one can obtain various scaling laws with exponent between zero (classical elasticity) and one (strain-gradient elasticity). Finally, we have shown that the overall behavior may be learned using a Fourier neural operator. We plan to build on this to study plasticity and other phenomena in future work.

Acknowledgements

We gratefully acknowledge the financial support of the Office of Naval Research through MURI award N00014-23-1-2654.

References

- [1] R. Adams and J. Fournier. *Sobolev Spaces, 2nd edition*. Academic Press, 2003.
- [2] E. C. Aifantis. The physics of plastic deformation. *International Journal of Plasticity*, 3:211–247, 1987.

- [3] G. Allaire, M. Briane, and M. Vanninathan. A comparison between two-scale asymptotic expansions and Bloch wave expansions for the homogenization of periodic structures. *SeMA Journal*, 73:237–259, 2016.
- [4] M. F. Ashby. The deformation of plastically non-homogeneous materials. *The Philosophical Magazine: A Journal of Theoretical Experimental and Applied Physics*, 21:399–424, 1970.
- [5] N. W. Ashcroft and N. D. Mermin. *Solid State Physics*. Cengage Learning, 1976.
- [6] N. Bakhvalov and G. Panasenko. *Homogenisation: Averaging Processes in Periodic Media*. Springer, 1989.
- [7] K. Bhattacharya, N. B. Kovachki, A. Rajan, A. M. Stuart, and M. Trautner. Learning Homogenization for Elliptic Operators. *SIAM Journal on Numerical Analysis*, 62:1844–1873, 2024.
- [8] C. Dahlberg and M. Ortiz. Fractional strain-gradient plasticity. *European Journal of Mechanics - A/Solids*, 75:348–354, 2019.
- [9] E. Di Nezza, G. Palatucci, and E. Valdinoci. Hitchhiker’s guide to the fractional Sobolev spaces. *Bulletin des Sciences Mathématiques*, 136:521–573, 2012.
- [10] D. Dunstan and A. Bushby. Grain size dependence of the strength of metals: The hall–petch effect does not scale as the inverse square root of grain size. *International Journal of Plasticity*, 53:56–65, 2014.
- [11] A. Eringen and D. Edelen. On nonlocal elasticity. *International Journal of Engineering Science*, 10:233–248, 1972.
- [12] A. C. Eringen. Linear theory of nonlocal elasticity and dispersion of plane waves. *International Journal of Engineering Science*, 10:425–435, 1972.
- [13] A. C. Eringen. Nonlocal polar elastic continua. *International Journal of Engineering Science*, 10:1–16, 1972.
- [14] A. C. Eringen. On differential equations of nonlocal elasticity and solutions of screw dislocation and surface waves. *Journal of Applied Physics*, 54:4703–4710, 1983.
- [15] N. Fleck and J. Hutchinson. A reformulation of strain gradient plasticity. *Journal of the Mechanics and Physics of Solids*, 49(10):2245–2271, 2001.
- [16] N. Fleck, G. Muller, M. Ashby, and J. Hutchinson. Strain gradient plasticity: Theory and experiment. *Acta Metallurgica et Materialia*, 42(2):475–487, 1994.
- [17] J. R. Greer and J. T. De Hosson. Plasticity in small-sized metallic systems: Intrinsic versus extrinsic size effect. *Progress in Materials Science*, 56:654–724, 2011.

- [18] M. E. Gurtin and L. Anand. A theory of strain-gradient plasticity for isotropic, plastically irrotational materials. Part I: Small deformations. *Journal of the Mechanics and Physics of Solids*, 53:1624–1649, 2005.
- [19] E. Hall. The deformation and ageing of mild steel: III Discussion of results. *Proceedings of the Physical Society. Section B*, 64:747–753, 1951.
- [20] N. Haskell. The dispersion of surface waves on multilayered media. *Bulletin of the Seismological Society of America*, 43:17–34, 1953.
- [21] D. P. Kingma and J. Ba. Adam: A Method for Stochastic Optimization. In *International Conference on Learning Representations (ICLR 2015)*, 2015.
- [22] L. Knopoff. A matrix method for elastic wave problems. *Bulletin of the Seismological Society of America*, 54:431–438, 1964.
- [23] N. Kovachki, Z. Li, B. Liu, K. Azizzadenesheli, K. Bhattacharya, A. Stuart, and A. Anandkumar. Neural operator: Learning maps between function spaces with applications to pdes. *Journal of Machine Learning Research*, 24:1–97, 2023.
- [24] J. Krumhansl. Some considerations of the relation between solid state physics and generalized continuum mechanics. In E. Kröner, editor, *Mechanics of Generalized Continua*, pages 298–311. Springer, 1967.
- [25] I. Kunin. Theory of elasticity with spatial dispersion one-dimensional complex structure. *Journal of Applied Mathematics and Mechanics*, 30:1025–1034, 1966.
- [26] Z. Li, N. Kovachki, K. Azizzadenesheli, B. Liu, K. Bhattacharya, A. Stuart, and A. Anandkumar. Fourier neural operator for parametric partial differential equations. In *International Conference on Learning Representations*, pages 1–16, 2021.
- [27] H. Moulinec and P. Suquet. A fast numerical method for computing the linear and nonlinear mechanical properties of composites. *Comptes Rendus de l’Académie des sciences. Série II. Mécanique, physique, chimie, astronomie*, 318:1417–1423, 1994.
- [28] H. Moulinec and P. Suquet. A numerical method for computing the overall response of nonlinear composites with complex microstructure. *Computer Methods in Applied Mechanics and Engineering*, 157:69–94, 1998.
- [29] H. Moulinec, P. Suquet, and G. W. Milton. Convergence of iterative methods based on Neumann series for composite materials: Theory and practice. *International Journal for Numerical Methods in Engineering*, 114:1103–1130, 2018.
- [30] Y. Mu, K. Chen, and W. Meng. Thickness dependence of flow stress of cu thin films in confined shear plastic flow. *MRS Communications*, 4:1–5, 09 2014.
- [31] Y. Mu, X. Zhang, J. Hutchinson, and W. Meng. Dependence of confined plastic flow of polycrystalline cu thin films on microstructure. *MRS Communications*, 20:1–6, 2016.

- [32] S. Müller and G. Francfort. Combined effects of homogenization and singular perturbations in elasticity. *Journal für die Reine und Angewandte Mathematik*, 454:1–36, 1994.
- [33] W. D. Nix and H. Gao. Indentation size effects in crystalline materials: a law for strain gradient plasticity. *Journal of the Mechanics and Physics of Solids*, 46(3):411–425, 1998.
- [34] A. Paszke, S. Gross, F. Massa, A. Lerer, J. Bradbury Google, G. Chanan, T. Killeen, Z. Lin, N. Gimelshein, L. Antiga, A. Desmaison, A. K. Xamla, E. Yang, Z. Devito, M. Raison Nabla, A. Tejani, S. Chilamkurthy, Q. Ai, B. Steiner, L. F. Facebook, J. B. Facebook, and S. Chintala. PyTorch: An Imperative Style, High-Performance Deep Learning Library. In *Neural Information Processing Systems (NeurIPS 2019)*, 2019. <https://pytorch.org/>.
- [35] N. J. Petch. The cleavage strength of polycrystals. *The Journal of the Iron and Steel Institute*, 174:25–28, 1953.
- [36] V. Smyshlyaev and K. Cherednichenko. On rigorous derivation of strain gradient effects in the overall behaviour of periodic heterogeneous media. *Journal of the Mechanics and Physics of Solids*, 48:1325–1357, 2000.
- [37] L. Tartar. *An introduction to Sobolev spaces and interpolation spaces*. Springer, 2007.
- [38] M. Thbaut, B. Audoly, and C. Lestringant. Fixing non-positive energies in higher-order homogenization. *Journal of the Mechanics and Physics of Solids*, 203:106168, 2025.
- [39] I. Vardoulakis, G. Exadaktylos, and E. Aifantis. Gradient elasticity with surface energy: Mode-III crack problem. *International Journal of Solids and Structures*, 33:4531–4559, 1996.
- [40] Z.-G. Zhou, J.-C. Han, and S.-Y. Du. Investigation of a Griffith crack subject to anti-plane shear by using the non-local theory. *International Journal of Solids and Structures*, 36:3891–3901, 1999.

Appendix

A Equilibrium and jump conditions

Assuming the elastic bar of length L and the jump at l , the energy can be written as

$$\mathcal{E}(u) = \frac{1}{2} \left(\int_0^l (Eu_x^2 + \kappa u_{xx}^2 - fu) dx + \int_l^L (Eu_x^2 + \kappa u_{xx}^2 - fu) dx \right). \quad (41)$$

The above expression for the energy is well defined only when u and u_x are continuous which implies that $[[u]]_{x=l} = [[u_x]]_{x=l} = 0$. Minimizing the energy *w.r.t* $u \implies \delta_u E =$

$\frac{\partial}{\partial \epsilon} E(u + \epsilon v) \Big|_{\epsilon=0} \forall v$ s.t $v(0) = 0$ and $v(L) = 0$. Substituting back in the energy integral, taking the derivative followed by the integration by parts, we get the following form

$$\int_0^L (((\kappa u_{xx})_x - (Eu_x))_x - f) v + [[(Eu_x - (\kappa u_{xx})_x) v]]_{x=l} + [[(\kappa u_{xx}) v_x]]_{x=l} + \kappa u_{xx} v_x \Big|_{x=L} - \kappa u_{xx} v_x \Big|_{x=0} = 0. \quad (42)$$

We can choose v such that each term in the above expression can be set equal to zero, therefore we get the equation of motion

$$((\kappa u_{xx})_x - (Eu_x))_x - f = 0, \quad (43)$$

jump conditions

$$[[Eu_x - (\kappa u_{xx})_x]]_{x=l} \text{ and } [[\kappa u_{xx}]]_{x=l}, \quad (44)$$

and two natural boundary conditions as follow

$$(\kappa u_{xx})_x(0) = 0 \text{ and } (\kappa u_{xx})_x(L) = 0. \quad (45)$$

B Formulas for the transfer matrix method

The function Φ in (10) is

$$\Phi = - \begin{pmatrix} e^{x/\lambda} \lambda^2 & e^{-x/\lambda} \lambda^2 & x & 1 \\ e^{x/\lambda} \lambda & -e^{-x/\lambda} \lambda & 1 & 0 \\ 0 & 0 & 1 & 0 \\ E \lambda^2 e^{x/\lambda} & E \lambda^2 e^{-x/\lambda} & 0 & 0 \end{pmatrix} \quad (46)$$

The particular solution in 10 for f constant is

$$\varphi^p = -\frac{1}{E} (x^2, x, x, \lambda^2 E)^T \quad (47)$$

while that for $f = e^{ikx}$ is

$$\varphi^p = -\frac{e^{ikx}}{Ek^2 + E\lambda^2 k^4} (1, ik, ik + i\lambda^2 k^3, -\lambda^2 k^2)^T \quad (48)$$

C Nonlocal elasticity

We start with the energetic formulation of linear strain gradient elasticity [12]

$$\mathcal{E}(u) = \frac{1}{2} \int_0^L A(Eu_x^2 + (K * u_x)^2 - fu) dx + \mathcal{B} \quad \text{where} \quad (K * v)(x) := \int_0^L K(x-y)v(y) dy. \quad (49)$$

The first variation is

$$\delta \mathcal{E} = \frac{d\mathcal{E}(u + \epsilon v)}{d\epsilon} \Big|_{\epsilon=0} = \int_0^L A(Eu_x v_x + (K * u_x)(K * v_x) - fv) dx + \mathcal{B}' \quad (50)$$

for a boundary term \mathcal{B}' . Now,

$$\begin{aligned}
\int_0^L (K * u_x)(K * v_x) dx &= \int_0^L \left((K * u_x)(x) \int_0^L K(x-y)v_x(y) dy \right) dx \\
&= \int_0^L \int_0^L ((K * u_x)(x)K(x-y)v_x(y)) dy dx \\
&= \int_0^L v_x(y) \left(\int_0^L (K * u_x)(x)K(x-y) dx \right) dy \\
&= \int_0^L v_x(y)K * (K * u_x)(y) dy
\end{aligned} \tag{51}$$

Substituting this back

$$\begin{aligned}
\delta\mathcal{E} &= \int_0^L A((Eu_x + K * (K * u_x)) v_x - fv) dx + \mathcal{B}' \\
&= - \int_0^L A((Eu_x + K * (K * u_x))_x + f) v dx + \mathcal{B}''
\end{aligned} \tag{52}$$

for a boundary term \mathcal{B}'' . Requiring that $\delta\mathcal{E} = 0$ for all v subject to boundary conditions leads to the governing equation (26).

D Fractional derivatives and fractional Laplacian

We define the energy in terms of the Gagliardo 2-semi-norm [9]:

$$\mathcal{E}(u) = \int_0^L A \left(\int_0^L \frac{1}{2} M\lambda^{2\alpha} \frac{(u'(x) - u'(y))^2}{|x-y|^{1+2\alpha}} dy - f(x)u(x) \right) dx + \mathcal{B} \tag{53}$$

where we use $'$ to denote derivative. Taking the first variation,

$$\begin{aligned}
\delta\mathcal{E} &= \left. \frac{d\mathcal{E}(u + \epsilon v)}{d\epsilon} \right|_{\epsilon=0} \\
&= \int_0^L A \left(\int_0^L M\lambda^{2\alpha} \left(\frac{u'(x) - u'(y)}{|x-y|^{1+2\alpha}} \right) (v'(x) - v'(y)) dy - f(x)v(x) \right) dx + \bar{\mathcal{B}} \\
&= \int_0^L A \left(2M\lambda^{2\alpha} v'(x) \int_0^L \left(\frac{u'(x) - u'(y)}{|x-y|^{1+2\alpha}} \right) dy - f(x)v(x) \right) dx + \bar{\mathcal{B}} \\
&= - \int_0^L A \left(2M\lambda^{2\alpha} \left(\int_0^L \left(\frac{u'(x) - u'(y)}{|x-y|^{1+2\alpha}} \right) dy \right)' + f(x) \right) v(x) dx + \tilde{\mathcal{B}}
\end{aligned} \tag{54}$$

where we integrate by parts in the final term. Requiring $\delta\mathcal{E} = 0$ for all v subject to the boundary condition provides the equilibrium equation in terms for the fractional Laplacian [9],

$$\left(\frac{2M\lambda^{2\alpha}}{C} (-\Delta)^\alpha u' \right)' + f = 0 \quad \text{where} \quad (-\Delta)^\alpha u := C \left(\frac{u'(x) - u'(y)}{|x-y|^{1+2\alpha}} \right) \tag{55}$$

where the constant C depends only α .